

## Grain structure and microtexture evolution during superplastic deformation of 5A90 Al–Li alloy

Pan ZHANG<sup>1,2</sup>, Ling-ying YE<sup>1,2</sup>, Xin-ming ZHANG<sup>1,2</sup>, Gang GU<sup>1,2</sup>, Hai-chun JIANG<sup>1,2</sup>, Yu-long WU<sup>1,2</sup>

1. School of Materials Science and Engineering, Central South University, Changsha 410083, China;

2. Key Laboratory of Nonferrous Materials Science and Engineering, Ministry of Education, Central South University, Changsha 410083, China

Received 17 October 2013; accepted 23 April 2014

**Abstract:** The microstructural evolution of banded 5A90 Al–Li alloy during superplastic deformation at 475 °C with an initial strain rate of  $8 \times 10^{-4} \text{ s}^{-1}$  was studied using EBSD technique. The results showed that, before deformation, the grain shape appeared to be banded, the most grain boundaries belonged to low-angle boundaries, and the initial sheet had a dominate of  $\{110\}\langle 112 \rangle$  brass texture. During deformation, there were grain growth, grain shape change, misorientation increasing and textural weakening. The fraction of high-angle boundaries increased rapidly once the flow stress reached the peak value. Corresponding deformation mechanism for various stages of deformation was suggested. Dislocation activity was the dominant mechanism in the first stage, then dynamic recrystallization occurred, and grain rotation was expected as an accommodation for grain boundary sliding (GBS). At large strains, GBS was the main mechanism.

**Key words:** 5A90 Al–Li alloy; superplasticity; microstructure; microtexture

### 1 Introduction

Generally, superplasticity is a characteristic of equiaxed, stable, fine-grained materials ( $<10 \text{ }\mu\text{m}$ ), consisting primarily of high-angle grain boundaries, when they are deformed in tension at relatively high temperatures [1,2]. The view of the microstructural development during superplastic deformation of the structural superplastic alloy is that equiaxed grains remain equiaxed even after large deformations, and there is a strongly promoted, but not unanimous view that grain boundary sliding (GBS) is the fundamental microstructural mechanism of superplasticity, even if accommodation mechanisms are often invoked to try to explain the high level of strain rate sensitivity of flow stress [3].

However, for several materials which initially contain elongated or banded microstructures, the flow behavior of the materials showing superplasticity by dynamic recrystallization was reported to be quite different from the GBS. For AA8090 alloy and Al–Cu–Zr alloy dislocation activity appears to be the

main mechanism during superplastic deformation [1,3]. Meanwhile, LYTTLE and WERT [4] considered that the mechanism of superplastic Al–Zr–Si alloy is the combination of subgrain rotation, subgrain neighbor switching and grain boundary sliding [4].

Although a number of literatures reported the superplasticity of the 5A90 Al–Li alloy sheets, most of them mainly concentrated on the development of the methods for the material with fine equiaxed grains and the optimization of superplastic condition [5–8]. The investigation on superplastic mechanism and micro-orientation evolution of the alloy sheets with an initial elongated grain microstructure is limited.

In this work, the evolution of microstructure and texture during superplastic deformation (SPD) of 5A90 Al–Li alloy sheets with elongated grains was examined, with the objective to find out how equiaxed grain microstructure and nearly random orientation evolve from elongated grains microstructure and strong brass (B) orientations, and then the superplastic mechanism of the alloy sheets was explored, which would provide experiment evidences and theoretical basis for the SPD mechanism of elongated grains.

## 2 Experimental

The material used was commercially produced 5A90Al–Li sheet of 2 mm in thickness, with a nominal composition (mass fraction, %) of Al–5.3Mg–2.12Li–0.11Zr–0.1Ti. The as-received sheet had been produced through a special thermomechanical processing which was established by ZHANG et al [9].

The SPD specimens had a gage length of 10.0 mm and a width of 6.0 mm. The tensile tests were performed on a RWS50 testing machine with the constant cross-head at an initial strain rate of  $8 \times 10^{-4} \text{ s}^{-1}$  and temperature of 475 °C. The elongation to failure for the particular alloy studied was 655 %, representing a true strain of 2.09. To study the process of the microstructure and microtexture evolution, the samples were stretched to the true strains of 0.18, 0.5, 0.56, 0.9, 1.16, and 1.27, respectively, which encompassed all major regions where the microstructure and texture were changed dramatically according to the true stress–strain curve.

The deformed samples for grain structure and microtexture analysis were performed on the rolling plane by SEM/EBSD technique. EBSD maps for microstructural characterization used a step size of 0.4  $\mu\text{m}$ , and regions of about  $100 \mu\text{m} \times 100 \mu\text{m}$  were examined. The EBSD data were analyzed using TSL-OIM software. Boundaries of misorientation less than  $1^\circ$  were ignored in order to remove noise. Boundaries of misorientation less than  $10^\circ$  were designed as low-angle boundaries and those of higher misorientation were as high-angle boundaries [10].

## 3 Results and discussion

### 3.1 True stress–strain curve

To study the evolution, the true stress–strain curve with the elongation of 655% is given in Fig. 1. The curve

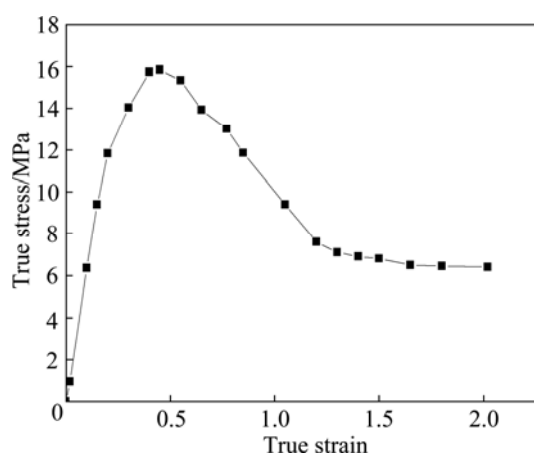


**Fig. 1** True stress–strain curve of 5A90 Al–Li alloy deformed at initial strain rate  $8 \times 10^{-4} \text{ s}^{-1}$  and temperature 475 °C

can be divided into three stages. In the initial stage, work hardening rate is quiet high; then the true stress reaches the peak value quickly and retains for a while; finally, it decreases quickly to a constant. This suggests that the process of the superplastic deformation of the initial sheets with elongated grains can be divided into three stages. In the initial stage ( $\epsilon \leq 0.45$ ), the true stress increases rapidly with a peak at the true strain of 0.45 and then dramatically decreases until true strain of 1.27 ( $0.45 < \epsilon < 1.27$ ). At larger true strains ( $\epsilon \geq 1.27$ ), the true stress tends to be independent of true strain. Therefore, we select the true strains of 0.18, 0.5, 0.56, 0.9, 1.16, and 1.27 to investigate the grain structure and microtexture evolution during superplastic deformation.

### 3.2 Misorientation evolution

The initial grains of 5A90 Al–Li alloy sheets used comprise an elongated grain microstructure as shown in Fig. 2(a), which suggests that the sheets are not recrystallized. And then, from the data of the distribution of misorientation angle of the rolling plane (Fig. 2(b)), it can be easily concluded that the initial sheet has a large fraction of low-angle boundaries.

Figure 3 shows the orientation maps for the 5A90 alloy. The initial banded microstructure, and the transformation into a more equiaxed grain structure,

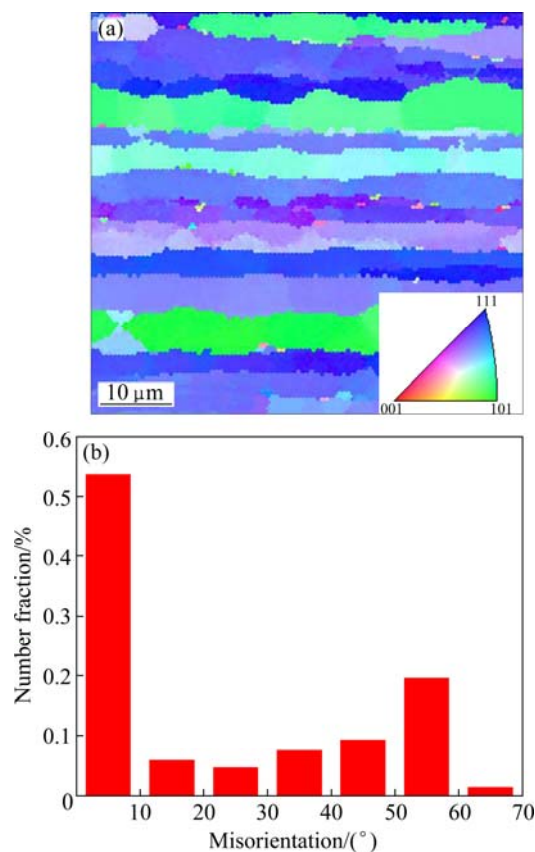


**Fig. 2** Orientation map (a) and misorientation angle distribution (b) of rolling plane

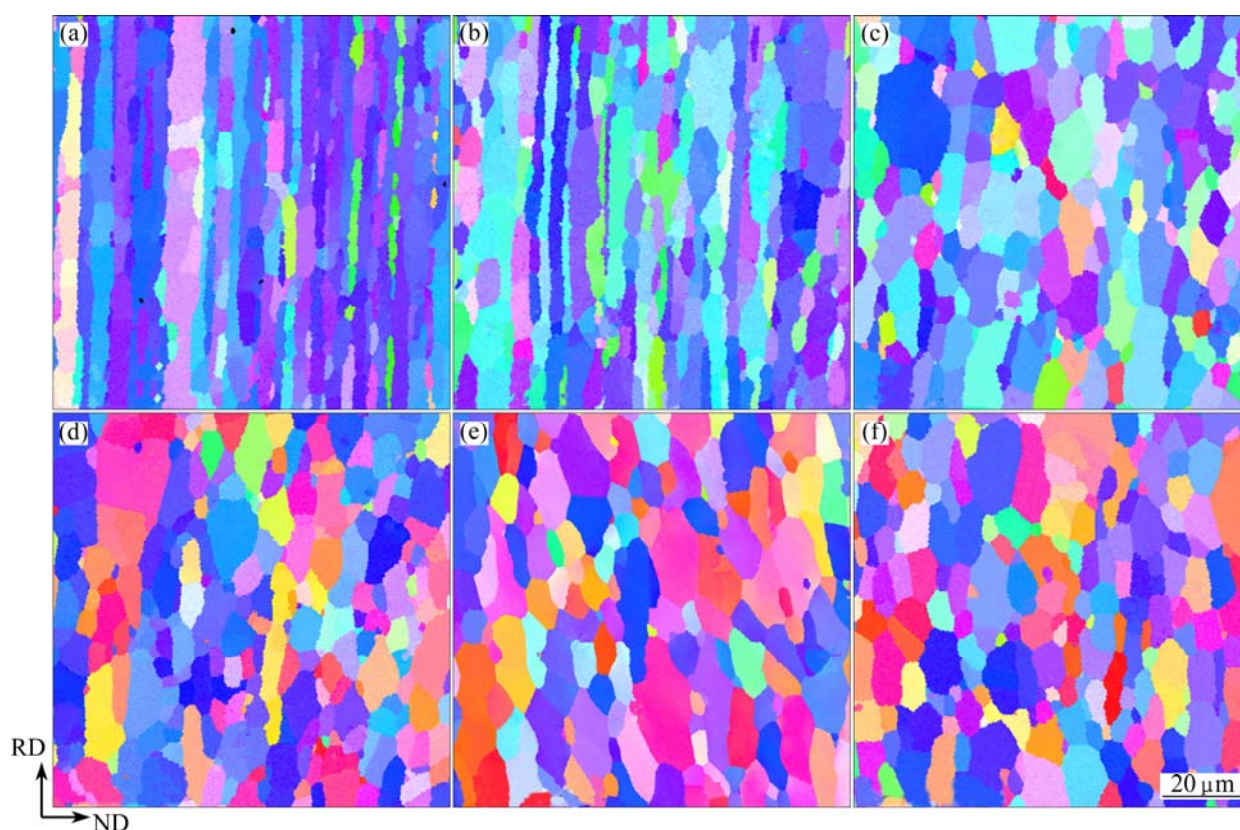


**Fig. 3** Orientation maps of samples deformed at different strains: (a)  $\varepsilon=0.18$ ; (b)  $\varepsilon=0.5$ ; (c)  $\varepsilon=0.56$ ; (d)  $\varepsilon=0.9$ ; (e)  $\varepsilon=1.16$ ; (f)  $\varepsilon=1.27$  (RD: Cross section of rolling direction; ND: Normal direction)

are clear. The evolution of grain size is rather complicated, mainly because it is not clear how a grain is defined in such a structure. Although the sampling used was clearly limited, some important trends in the microstructural evolution can be observed. There is a growth in  $\lambda_{ND}$ , but a reduction at intermediate strains in  $\lambda_{RD}$ .

At the true strain of 0.18, the microstructure, combined with banded grains and a few recrystallized grains, was not noticeably different from that of initial sample. At the strains of 0.5 and 0.56, some elongated-recrystallized grains were observed, but they were far from being fully recrystallized. At the higher strains of 0.9 and 1.16, the banded structure was substantially replaced by a more equiaxed and uniform grain structure. At a strain of 1.27, the microstructure resembled the appearance of a nearly equiaxed recrystallized fine grain structure.

Misorientation angles between contiguous grains and subgrains along the RD and the corresponding misorientation distribution histograms are presented in Fig. 4. A gradual shift from an initially high population (~46%) of low-angle ( $<10^\circ$ ) grain boundaries in the initial sheet to relatively high-angle ( $>10^\circ$ ) grain boundaries can be seen. During superplastic deformation, the low-angle boundaries decreased and high-angle

boundaries increased. At the strain of 1.27, the grain structure appeared nearly equiaxed, and the misorientation distribution also appeared that high-angle boundaries are in a relatively large fraction. With the change of grain shape and distributions of misorientation, it can be concluded that continuous recrystallization occurs during the second stage, which can account for the drop of flow stress through the maximum stress point.

As well as the dynamic grain growth and misorientation distribution, a major factor in the microstructural development is the evolution of crystallographic texture. Microtexture information derived from the analysis of the orientation data is presented in the form of (100), (110), (111) pole figures in Fig. 5 for samples with strains of 0.18 to 1.27. For the strain level of 0.18, a strong  $\{110\} \langle 112 \rangle$  brass texture, which is the dominant plane strain hot deformation texture for aluminum alloys, was observed, according to the pole figures shown in Fig. 5. The pole figures also showed that the strong brass texture persisted at the strain of 0.5. In contrast, the pole figure for the strain of 1.27 appeared much diffused with a random texture. Thus, along with the increase in the highly misoriented boundaries, a randomization of the local texture occurred with increasing strain.

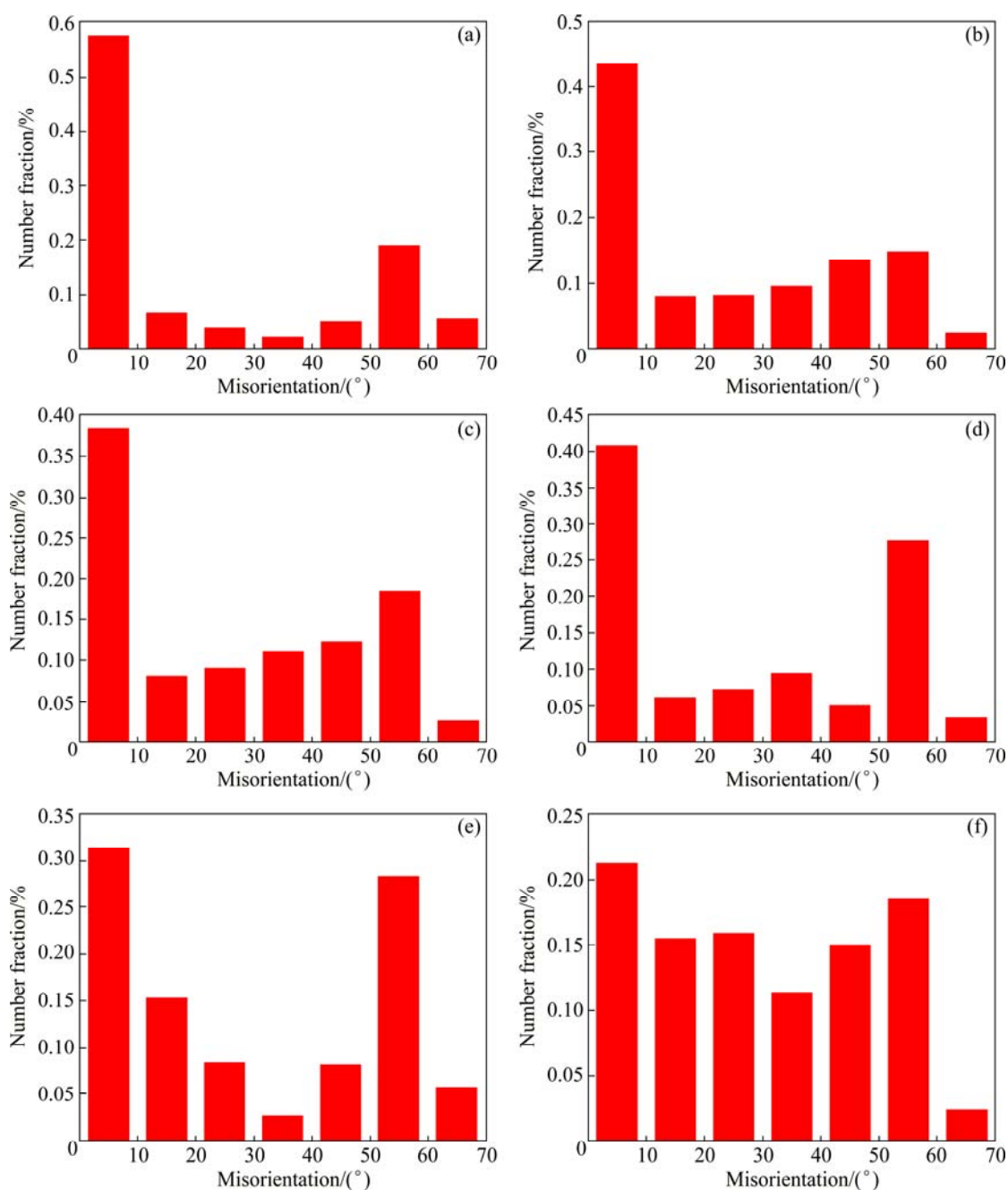


**Fig. 4** Misorientation distributions of samples deformed at different true strains: (a)  $\varepsilon=0.18$ ; (b)  $\varepsilon=0.5$ ; (c)  $\varepsilon=0.56$ ; (d)  $\varepsilon=0.9$ ; (e)  $\varepsilon=1.16$ ; (f)  $\varepsilon=1.27$

### 3.3 Superplastic mechanism

In most superplastic deformation studies of materials with similar starting microstructure, deformation induced continuous recrystallization (DICR) and grain boundary sliding (GBS) are often proposed to explain the evolution of grain and microtextural features as observed in the present study [11–13]. However, specific mechanism during the process of DICR is still unclear. The initial microstructure of 5A90 Al–Li alloy sheets used comprises elongated grains, which are the characteristics of the deformation microstructure.

In the initial stage of SPD, true stress increases

rapidly with increasing true strain. There are two possibilities for the case [14]: grain widening during SPD, and the conventional dislocation-related strain hardening. By comparison of true stress obtained from experiment with calculation according to the deduced equation  $\sigma_1 = d_1 \sigma_0 / d_0$  [15], where  $d_0$  and  $d_1$  are the grain sizes,  $\sigma_0$  and  $\sigma_1$  are the stresses at the onset of plastic strain ( $\varepsilon_0$ ) and at any selected strain level  $\varepsilon_1$ , respectively. (Fig. 6), it can be seen that grain widening is not the main reason for the rapid increasing true stress as the true stress between experimental and calculated data has a enormous range. Therefore, the dislocation activity



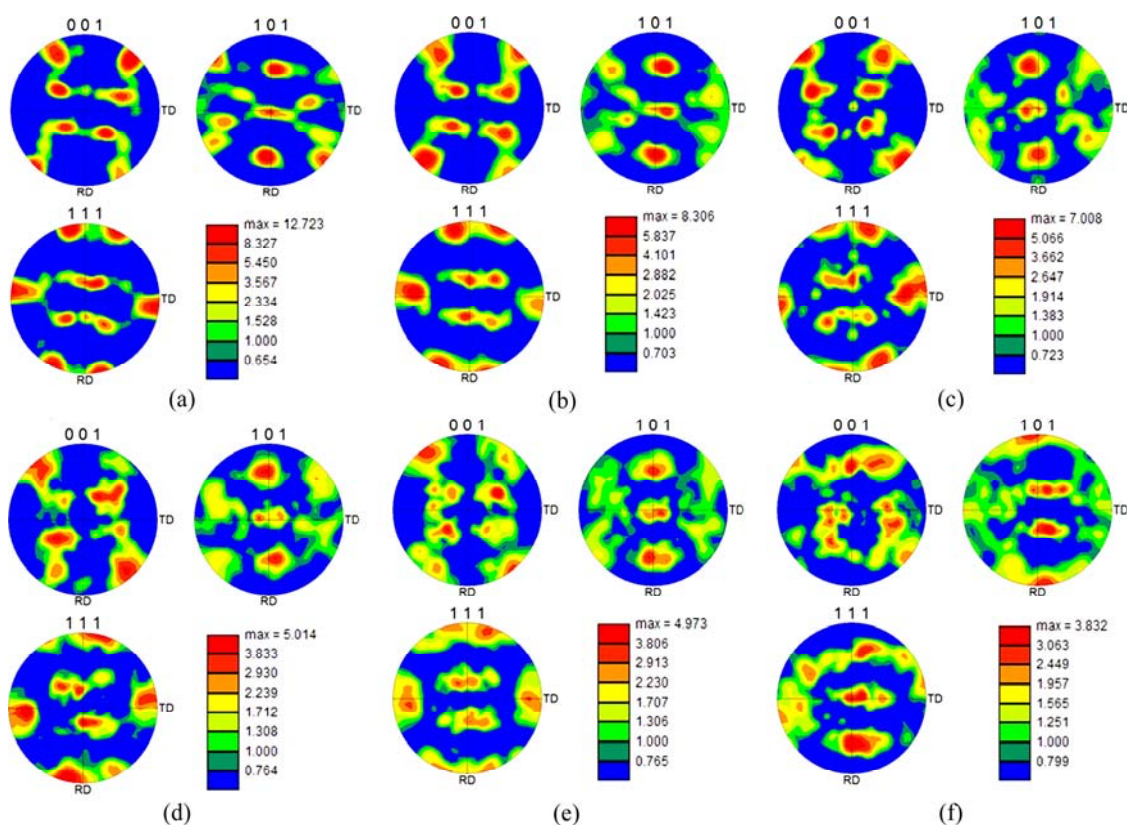


Fig. 5 Pole figures of samples deformed at different true strains: (a)  $\varepsilon=0.18$ ; (b)  $\varepsilon=0.5$ ; (c)  $\varepsilon=0.56$ ; (d)  $\varepsilon=0.9$ ; (e)  $\varepsilon=1.16$ ; (f)  $\varepsilon=1.27$

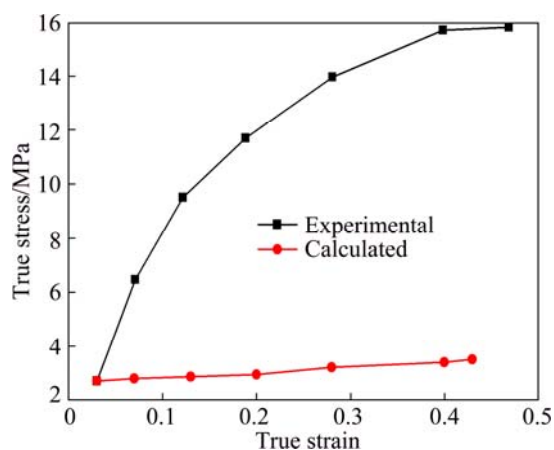


Fig. 6 Comparison of true stress obtained from experiment with calculation data

might be involved in this stage, which was also suggested in Refs. [14,15]. Meanwhile, the fraction of low-angle grain boundary decreased as well as the intensity of texture.

At the true strains from 0.45 to 1.27, the true stress decreases dramatically, which may come from the gradual decrease in strain rate, and the changes in microstructure of the sheets. In this stage, the initial elongated deformation microstructures are characterized by grain subdivision in differently oriented regions with low orientation density [11]. In the initial stage of SPD,

the orientation density increases due to the dislocation activity [14]. Thus, dynamic recrystallization occurs, by which GBS is possibly operative and the grain rotation occurs as an accommodation to GBS.

At larger strains ( $\varepsilon \geq 1.27$ ), grain structure appears to be equiaxed, the misorientation increased and the fraction of high-angle boundaries is much higher than that of low-angle grain boundaries, and the corresponding pole figure appeared much diffused with a random texture. Figure 7 shows the Ashby–Verrall superplastic model [16]. The characteristic of it is the fact that the grain shape does not change during stretching. Therefore, at this stage the superplastic mechanism is dominated by GBS and grain boundary migration, which makes contribution to grain growth and becomes the accommodation process.

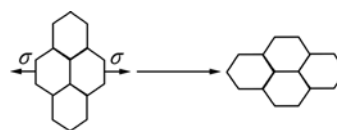


Fig. 7 Ashby–Verrall model [16]

## 4 Conclusions

1) Tensile strain of initial 5A90 sheet material parallel to the rolling direction at 475 °C using a constant

strain rate of  $8 \times 10^{-4} \text{ s}^{-1}$  showed that the microstructure, which initially was heavily banded and contained a high portion of low-angle boundaries, changed progressively during deformation to a relatively equiaxed structure with a large fraction of high-angle grain boundaries.

2) The initial texture had a dominant texture centered on  $\{110\}\langle 112 \rangle$  and tensile deformation led to a reduction in texture intensity. At the strain of 1.27, the corresponding pole figure and misorientation distribution appeared to be random.

3) The analysis of orientation/misorientation and the stress-strain curve show that dislocation slip is the main mechanism in the initial straining stage before the formation of high angle grain boundaries, and that grain boundary sliding is the dominant mechanism with equiaxed grains.

## References

- [1] BATE P S, RIDLEY N, ZHANG B. Mechanical behavior and microstructural evolution in superplastic Al–Li–Mg–Cu–Zr AA8090 [J]. *Acta Materialia*, 2007, 55(15): 4995–5006.
- [2] SAKAI G, HORITA Z, LANGDON T G. Grain refinement and superplasticity in an aluminum alloy processed by high-pressure torsion [J]. *Materials Science and Engineering A*, 2005, 393(1–2): 344–351.
- [3] SOTOUEH K, BATE P S. Diffusion creep and superplasticity in aluminium alloys [J]. *Acta Materialia*, 2010, 58(15): 1909–1920.
- [4] LYTTLE M T, WERT J A. Modelling of continuous recrystallization in aluminium alloys [J]. *Journal of Materials Science*, 1994, 29(12): 3342–3350.
- [5] ZHANG Xin-ming, YE Ling-ying, DU Yu-xuan, LUO Zhi-hui. Particle stimulated nucleation of recrystallization in 01420 Al–Li alloy [J]. *Journal of Central South University: Science and Technology*, 2007, 38(1): 19–23. (in Chinese)
- [6] ZHANG Xin-ming, ZHENG Da-wei, YE Ling-ying, TANG Jian-guo. Superplastic deformation behavior and mechanism of 1420 Al–Li alloy sheets with elongated grains [J]. *Journal of Central South University of Technology*, 2010, 17(4): 659–665.
- [7] MAZILKIN A A, MYSHLYAEV M M. Microstructure and thermal stability of superplastic aluminium-lithium alloy after severe plastic deformation [J]. *Journal of Materials Science*, 2006, 41(12): 3767–3772.
- [8] ZHANG Xin-ming, YE Ling-ying, LIU Ying-wei, DU Yu-xuan, LUO Zhi-hui. Formation mechanism of gradient-distributed particles and their effects on grain structure in 01420 Al–Li alloy [J]. *Journal of Central South University of Technology*, 2008, 15(2): 147–152.
- [9] YE Ling-ying. Fine grain deformation behavior and mechanism of 5A90Al–Li alloy [D]. Changsha: Central South University, 2010. (in Chinese)
- [10] HUANG Y, HUMPHREYS F J. Measurements of subgrain growth in a single-phase aluminum alloy by high-resolution EBSD [J]. *Material Characterization*, 2001, 47: 235–240.
- [11] DOHERTY R D, HUGHES D A, HUMPHREYS F J, JONAS J J, JUUL JENSEN D, KASSNER M E, KING W E, MCNELLEY T R, MCQUEEN H J, ROLLETT A D. Current issues in recrystallization: A review [J]. *Materials Science and Engineering A*, 1997, 238(2): 219–274.
- [12] LIU F C, XUE P, MA Z Y. Microstructural evolution in recrystallized and unrecrystallized Al–Mg–Sc alloys during superplastic deformation [J]. *Materials Science and Engineering A*, 2012, 547: 55–63.
- [13] MUKHOPADHYAY A K, KUMAR A, RAVEENDRA S, SAMAJDAR I. Development of grain structure during superplastic deformation of an Al–Zn–Mg–Cu–Zr alloy containing Sc [J]. *Scripta Materialia*, 2011, 64(5): 386–389.
- [14] LIU J, CHAKRABARTI D J. Grain structure and microtexture evolution during superplastic forming of a high strength Al–Zn–Mg–Cu alloy [J]. *Acta Materialia*, 1996, 44(12): 4647–4661.
- [15] FAN W J, KASHYAP B P, CHATURVEDI M C. Anisotropy in flow and microstructural evolution during superplastic deformation of a layered-microstructured AA8090 Al–Li alloy [J]. *Materials Science and Engineering A*, 2003, 349: 166–182.
- [16] WU Shi-chun. Theories on superplastic deformation [M]. Beijing: National Defence Industry Press, 1997. (in Chinese)

# 5A90 Al–Li 合金超塑性变形过程中的显微组织及微观织构演变

张盼<sup>1,2</sup>, 叶凌英<sup>1,2</sup>, 张新明<sup>1,2</sup>, 顾刚<sup>1,2</sup>, 蒋海春<sup>1,2</sup>, 吴豫陇<sup>1,2</sup>

1. 中南大学 材料科学与工程学院, 长沙 410083;

2. 中南大学 有色金属材料科学与工程教育部重点实验室, 长沙 410083

**摘要:** 通过采用电子背散射衍射技术研究具有扁平状组织的 5A90 Al–Li 合金板材在变形条件  $475^\circ\text{C}$ 、 $8 \times 10^{-4} \text{ s}^{-1}$  时的显微组织演变。结果表明, 在进行超塑性变形前, 其显微组织表现为扁平状组织, 具有大量的小角度晶界, 且初始板材具有明显的黄铜织构  $\{110\}\langle 112 \rangle$ 。在变形过程中发生了晶粒的长大、晶粒形貌的改变、晶粒取向差的增大以及织构的弱化, 而且大角度晶界的含量在流动应力到达最大值后开始逐渐增加。同时, 对不同阶段的相关变形机制进行了讨论。超塑性变形初始阶段的主要变形机制为位错运动, 随着变形的进行而开始发生动态再结晶, 晶粒旋转作为晶界滑移的主要协调机制。在超塑性拉伸的最后大应变阶段, 晶界滑移是主要的变形机制。

**关键词:** 5A90 Al–Li 合金; 超塑性; 显微组织; 显微织构

(Edited by Xiang-qun LI)